iScience

CellPress
OPEN ACCESS

Article

Crotonylation sensitizes IAPi-induced disruption of latent HIV by enhancing p100 cleavage into p52

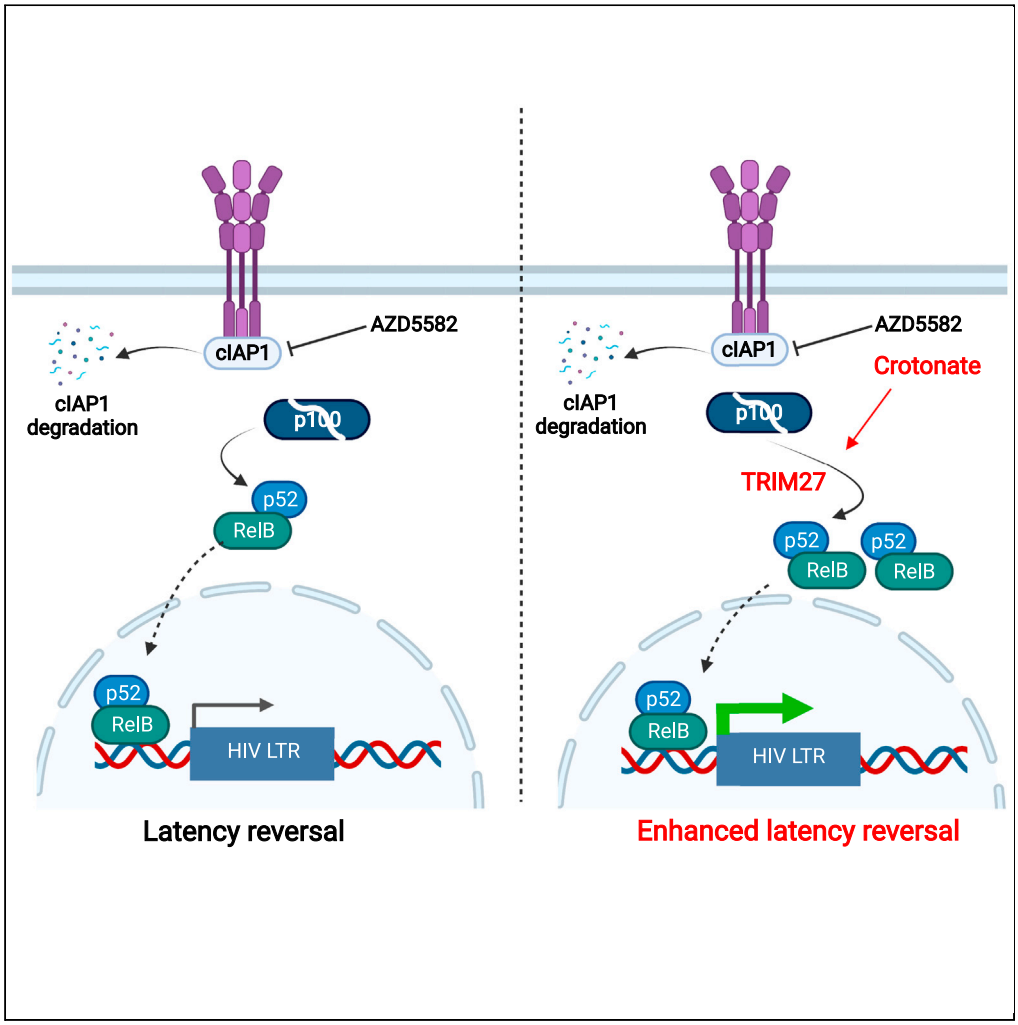

Dajiang Li, Morgan G. Dewey, Li Wang, ..., Nancie M. Archin, David M. Margolis, Guochun Jiang

guochun_jiang@med.unc.edu

Highlights

Crotonylation enhances IAPi (AZD5582)-induced HIV latency reversal

Crotonylation augments the p100 cleavage into p52

TRIM27 is involved in the enhanced p100 cleavage

TRIM27 Knockdown reduced p100/p52 levels and inhibits HIV latency reversal

Li et al., iScience 25, 103649
January 21, 2022
https://doi.org/10.1016/j.isci.2021.103649

iScience

CellPress
OPEN ACCESS

Article

Crotonylation sensitizes IAPi-induced disruption of latent HIV by enhancing p100 cleavage into p52

Dajiang Li,[1] Morgan G. Dewey,[1] Li Wang,[2] Shane D. Falcinelli,[1,3] Lilly M. Wong,[1] Yuyang Tang,[1] Edward P. Browne,[1,3,4] Xian Chen,[2] Nancie M. Archin,[1,4] David M. Margolis,[1,3,4] and Guochun Jiang[1,2,5,*]

SUMMARY

The eradication of HIV infection is difficult to achieve because of stable viral reservoirs. Here, we show that crotonylation enhances AZD5582-induced noncanonical NF-κB (ncNF-κB) signaling, further augmenting HIV latency reversal in Jurkat and U1 cell line models of latency, HIV latently infected primary CD4+ T cells and resting CD4+ T cells isolated from people living with HIV. Crotonylation upregulated the levels of the active p52 subunit of NF-κB following AZD5582. Biochemical analyses suggest that the ubiquitin E3 ligase TRIM27 is involved in enhanced p100 cleavage to p52. When TRIM27 was depleted, AZD5582-induced HIV latency reversal was reduced. TRIM27 small interfering RNA (siRNA) knockdown reduced both p100 and p52 levels without inhibiting p100 transcription, indicating that TRIM27 not only acts on p100 cleavage but also may impact p100/p52 stability. These observations reveal the complexity of HIV transcriptional machinery, particularly of NF-κB.

INTRODUCTION

Current antiretroviral therapy (ART) effectively inhibits viral replication and slows disease progression but fails to eliminate the extremely stable HIV reservoirs in patients (Chun et al., 1997; Finzi et al., 1997; Wong et al., 1997). Over the past decades, enormous efforts have been made to directly attack latent HIV-1 (HIV) in which HIV latency reversal agents (LRAs) (Archin et al., 2012; Cary et al., 2016; Karn, 2011; Sengupta and Siliciano, 2018) are combined with immune enhancing methods for effective clearance of viral reservoirs. Many LRAs have been tested to target mechanisms of HIV latency, including epigenetic regulators to remodel the chromatin environment at the HIV LTR, protein kinase C agonist (PKCa) to induce activation of canonical NF-κB (cNF-κB) signaling, or bromodomain inhibitor (BETi) to inhibit BRD4 in the TAR/Tat/P-TEFb complex (Archin et al., 2012, 2014; Banerjee et al., 2012; Friedman et al., 2011; Jiang et al., 2007, 2014; Karn, 2011; Karn and Stoltzfus, 2012; Kessing et al., 2017). Among all these LRAs, PKCa has been shown to be the strongest in *ex vivo* studies (Darcis et al., 2015; Jiang and Dandekar, 2015; Jiang et al., 2015; Laird et al., 2015; Spina et al., 2013). Therefore, several preclinical and pilot clinical studies have been carried out to test their potential clinical relevance (Gutierrez et al., 2016; Marsden et al., 2017). Although PKCa can disrupt latent HIV *ex vivo* and in a topical skin lesion model of latency *in vivo* (Jiang et al., 2015, 2019; Sloane et al., 2020), concerns remain regarding side effects from cellular toxicities and immune activation following systemic administration. Alternative strategies for the activation of NF-κB are being pursued.

In addition to the canonical NF-κB (cNF-κB) pathway, other NF-κB subpathways regulate gene transcription *via* NF-κB DNA binding sites (Wong and Jiang, 2021). These include noncanonical NF-κB (ncNF-κB) and atypical NF-κB pathways (Sun, 2012; Sun and Ley, 2008; Wong and Jiang, 2021). For example, whereas RelA/p50 is released from IκB after IκB phosphorylation and ubiquitination during canonical NF-kB signaling, the activation of ncNF-κB is dependent on the cleavage of p100 into p52 after p100 phosphorylation by NF-κB activating kinase (NIK) (Sun, 2012). Targeting the noncanonical NF-κB pathway has recently been explored for the disruption of HIV latency (Pache et al., 2015). siRNA knockdown identified one essential negative regulator of ncNF-κB, BIRC2/cIAP1, as an inhibitor of HIV transcription and promoter of HIV (Pache et al., 2015). When targeted by the inhibitor of apoptosis (IAP) inhibitor small molecules (IAPi, also known as SMAC mimetics), cIAP1 auto-ubiquitinates and is degraded by the proteasome. The loss of cIAP1 enables NIK to accumulate and phosphorylate p100, leading to cleavage and release of

[1]UNC HIV Cure Center, Institute of Global Health and Infectious Diseases, The University of North Carolina at Chapel Hill, 120 Mason Farm Rd, Genetic Medicine Building, Room 2111, Chapel Hill, NC 27599-7042, USA

[2]Department of Biochemistry and Biophysics, The University of North Carolina at Chapel Hill, Chapel Hill, NC 27599-7042, USA

[3]Department of Microbiology and Immunology, The University of North Carolina at Chapel Hill, Chapel Hill, NC 27599-7042, USA

[4]Department of Medicine, The University of North Carolina at Chapel Hill, Chapel Hill, NC 27599-7042, USA

[5]Lead contact

*Correspondence: guochun_jiang@med.unc.edu

https://doi.org/10.1016/j.isci.2021.103649

the active subunit p52, which translocates to the nucleus to form a transcriptional activator in complex with RelB.

Most recently, it was reported that the induction of ncNF-κB by the IAPi AZD5582 (Hennessy et al., 2013) induced HIV expression in both HIV-infected, ART-suppressed humanized mice and SIV-infected, ART-suppressed macaques (Hennessy et al., 2013; Nixon et al., 2020). Of note, ncNF-κB signaling tends to be slower and the induction of ncNF-κB by IAPi is more selective, inducing only a few hundred genes in contrast to the thousands of host genes modulated by the cNF-κB, MAPK, and calcineurin signaling induced by PKCa (Nixon et al., 2020; Sun, 2017).

In a previous study, we found that protein crotonylation is involved in the transcription of HIV and/or latency reversal, which significantly enhanced canonical NF-κB activation-induced latency reversal compared with other signaling pathways associated with HIV latency (Jiang et al., 2018). In this study, we aimed to understand whether the activation of ncNF-κB can be improved by protein crotonylation to allow accelerated clearance of latent HIV. We found that the treatment with sodium crotonate enhanced HIV transcription from latency induced by IAPi. This was observed in Jurkat HIV latency models, the promonocyte HIV latency model U1 cells, primary CD4+ T cell model of latency and resting CD4+ T cells isolated from ART-suppressed people living with HIV (PLWH). We observed that crotonylation augmented the levels of p52 induced by AZD5582 in the Jurkat model of HIV latency, a crucial step for the activation of the ncNF-κB pathway. As the induction of crotonylation is expected to induce HIV expression *via* crotonylation mechanisms (Jiang et al., 2018), we further sought to understand this unexpected effect on p52. Proteomic analysis identified TRIM27 as an important target of protein crotonylation in response to crotonate, whereas TRIM27 siRNA knockdown inhibited latency reversal and dampened p100/p52 protein levels. TRIM27 could be involved in HIV transcription through its known interaction with USP7, thereby regulating p100 cleavage to enhance ncNF-κB signaling for latency reversal.

RESULTS

Protein crotonylation sensitizes IAPi-induced disruption of latent HIV in a broad range of HIV latency models

Previously, we showed that the metabolic induction of protein crotonylation in cells supplemented with sodium crotonate (NaCr) reversed HIV latency through increased expression of the crotonyl-CoA–producing enzyme acyl-CoA synthetase short-chain family member 2 (ACSS2). In this setting, the induction of latent HIV was further enhanced by PEP005, a canonical NF-κB activator. To determine if increased crotonylation also augmented ncNF-κB signaling and HIV latency reversal induced by IAPi, we tested the IAPi, AZD5582, in the Jurkat cell line models of latency, 2D10 and J-Lat A1 cells (Figure 1). Consistent with our previous observations (Jiang et al., 2018), crotonylation induction alone reactivated latent HIV with no significant toxicity in the 2D10 (Figures 1A and S1B) and J-Lat A1 cells (Figures 1D and 1E). Importantly, simultaneous induction of protein crotonylation by NaCr and activation of ncNF-κB signaling by AZD5582 synergistically reactivated HIV from latency with no toxicity (Figures 1A–1F). A similar synergistic effect was also observed in the J-Lat 10.6 model of latency (Figures S1A and S1B). [Crotonylation enhances AZD5582-induced HIV transcription from latency in J-Lat 10.6 model of HIV latency], related to Figure 1).

To confirm the above observations in cells that were not transformed, we repeated the experiments in a previously reported primary CD4+ T cell model of latency (Bradley et al., 2018). Briefly, CD4+ T cells were isolated from HIV-negative donors and infected with GFP-tagged NL4.3Δ6 HIV. A few days later, GFP + positive cells were sorted by flow cytometry and co-cultured on H80 feeder cells to allow descent into latency. GFP- CD4+ T cells were FACS-sorted, expanded and allowed to return to a quiescent state. The latently infected population of primary CD4+ T cells was reactivated by anti-CD3/CD28. These cells gradually returned to latency after anti-CD3/CD28 removal (Figure 2A). This primary CD4+ T cell model of latency (CD4+ T cells were from donor E117) was treated with 30 mM NaCr, 100 nM AZD5582, or with a combination of 30 mM NaCr with 100 nM AZD5582 for 24 h (Nixon et al., 2020). A higher dosage of AZD5582 was used to disrupt latent HIV in primary CD4+ T cells (Nixon et al., 2020). We measured GFP by flow cytometry and found that the induction of crotonylation in this model resulted in the induction of expression of latent HIV. Unlike crotonate, in this primary cell model the induction of ncNF-κB activation by AZD5582 alone had limited effects on latency disruption 48 h post-treatment, compared to control treatment. However, the percentage of GFP-positive cells was significantly increased in cells exposed to combination of AZD5582 with crotonate, compared with AZD5582 treatment alone (Figures 2B and 2C) with no

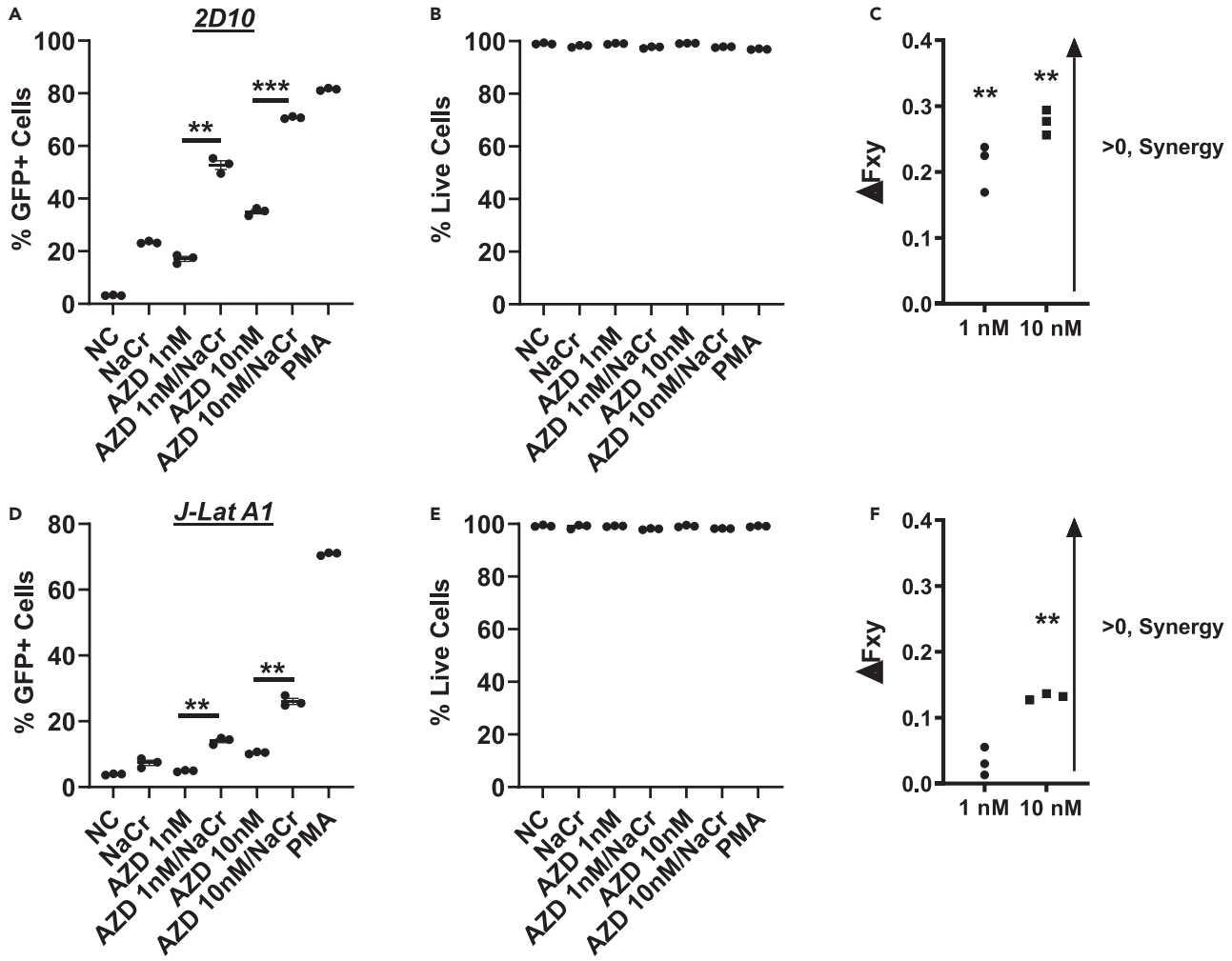

Figure 1. Crotonylation enhances AZD5582-induced HIV reactivation in HIV latency models

(A–C) 2D10 cells were treated with 1–10 nM AZD5582 (AZD), 40 mM NaCr, 50 ng/mL phorbol 12-myristate 13-acetate (PMA), or AZD/NaCr in combination. Cells were harvested 24 h posttreatment. Percentage of GFP and cell viability was analyzed by flow cytometry, whereas synergy of reactivation was determined by Bliss independence assay.

(D–F) J-Lat A1 cells were similarly treated as in 2D10 cells. Percentage of GFP and cell viability was analyzed by flow cytometry, whereas synergy of reactivation was determined by Bliss Independent assay. **, $p < 0.01$; ***, $p < 0.001$, compared with AZD alone and analyzed by two-tailed T test. Synergy of latency reversal was determined by Bliss independence analysis (n = 3). Data are represented as mean ± SEM.

significant induction of toxicity. This was similarly observed in another primary CD4+ T cell model of latency (CD4+ T cells were from donor E47) (Figure 2D–2F). Interestingly, unlike in E117, there was synergistic reactivation between NaCr and AZD5582, although not strong, indicating that the degree of latency reversal enhancement may vary among primary CD4+ T cell models of latency. Taken together, these data indicate that simultaneous crotonylation and ncNF-κB signaling augments the reactivation of latent HIV.

Crotonylation enhances latency reversal elicited by other IAPi

Other IAPis, such as birinapant, have been developed for use in oncology (Condon et al., 2014). We examined the effect of birinapant in combination with crotonate to see whether the synergistic latency reversal induced by crotonate is a specific property of AZD5582 (Figures 3 and S2. [Cellular viability during IAPi treatment in HIV latency models], related to Figure 3). We first compared the latency reversal activity of these two IAPis. In both 2D10 and J-Lat A1 cells, AZD5582 was more effective in latency reversal than Birinapant. Notably, even at 1 nM, AZD5582 was able to induce transcription of HIV compared with control. Surprisingly, in the promonocytic U1 model of latency, IAPi induced little latency reversal, except with a

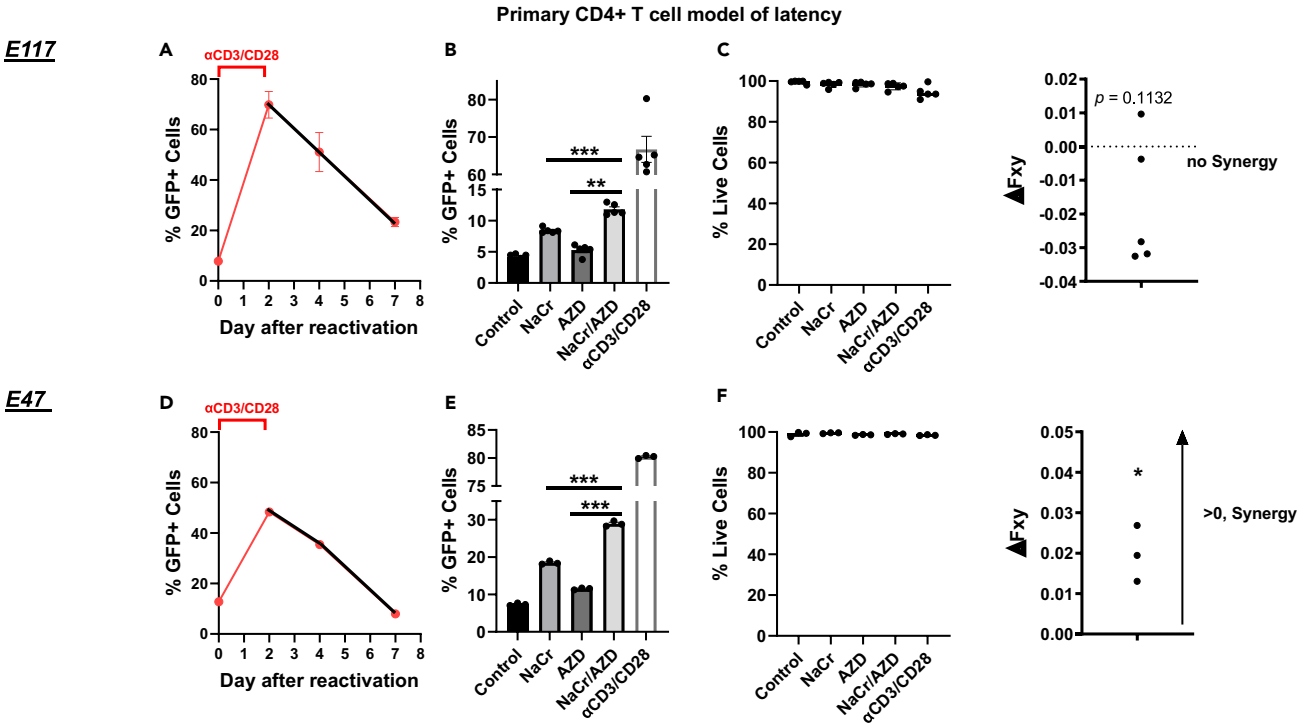

Figure 2. Crotonylation enhances AZD5582-induced HIV latency reversal in the primary CD4+ T cell model of latency

(A–C) Primary CD4+ T cell model of latency generated from HIV negative donor E117 was activated by anti-CD3/CD28 beads for days, which returned to latency after antibodies/beads removal (n = 3). This model was treated with 100 nM AZD5582 (AZD), or 30 mM NaCr or in combination for 48 h. Percentage of GFP positive and cell viability were analyzed by flow cytometry. Synergy reactivation was determined by Bliss independent analysis.

(D–F), Primary CD4+ T cell model of latency generated from HIV negative donor E47 was similarly prepared, LRA treated and analyzed as in (A–C). *, $p < 0.05$; **, $p < 0.01$; ***, $p < 0.001$, analyzed by two-tailed T test (n = 3–5). Data are represented as mean ± SEM.

high concentration of 500 nM (Figure 3A). Next, we compared IAPi latency reversal in combination with crotonate. Here, 10 nM was selected so that roughly comparable latency reversal could be seen in the different cell models. In combination, crotonate was able to increase the latency reversal induced by IAPi, even in the U1 cell model of latency. However, overall, crotonate similarly augmented the effect of AZD5582 and Birinapant (Figure 3B). Therefore, although latency reversal activity differs between IAPis and across HIV latency models, IAPi latency reversal appears broadly enhanced by crotonate.

Further, it has been reported that high concentrations of IAPi may be able to directly induce cell death of HIV + memory CD4+ T cells (Campbell et al., 2018). However, we did not observe cell death in the population of GFP + cells treated with IAPi alone in 2D10 cell model of latency (Figures 4A–4C). Notably, even at high dosages where latency reversal by both compounds reached >50% of the cells, AZD5582 failed to induce Annexin V in GFP + cells. However, an enhancement of Annexin V+ cells was observed in a minority of GFP + cells when treated with birinapant in combination with crotonate. Similarly, no significant induction of apoptosis was observed in the GFP + primary CD4+ T cell model of latency, with either single agent or combination treatment (Figure S3. [Crotonylation and IAPi treatments induce limited apoptosis in the primary CD4+ T cell model of latency], related to Figure 4), suggesting that crotonate may produce subtle differences in the induction of cellular pathways by different IAPIs, even when HIV latency reversal effects measured appear similar (Figures 4B and 4C).

Crotonate enhances IAPi-induced cleavage of p100 into p52

One of the key steps in the activation of the ncNF-κB signaling pathway is the cleavage of p100 into p52, which occurs after phosphorylation of p100 by NIK. The latter is normally degraded *via* cIAP1 ubiquitination (Sun, 2017). IAPi such as AZD5582 bind to cIAP1 to induce its auto-ubiquitination and degradation, which allows NIK to accumulate (Figure 5A). This leads to reactivation of latent HIV by induction of p100 cleavage into p52 and ncNF-κB signaling (Nixon et al., 2020). We noted with interest that crotonate was able to

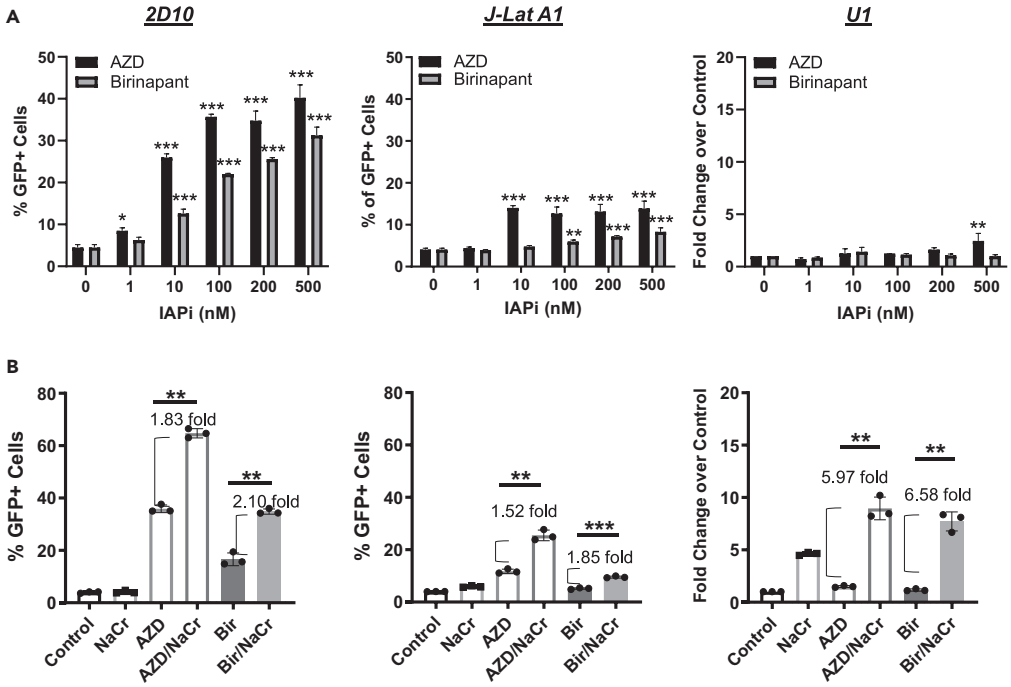

Figure 3. Latency reversal by IAPi with distinct chemical structures

(A) 2D10, J-Lat A1 and U1 cells were treated with different doses of AZD5582 (AZD) or Birinapant for 24 h. Percentage of GFP positive in 2D10 and J Lat A1 cells was analyzed by flow cytometry, whereas HIV RNA in U1 cells was analyzed by qPCR (n = 3). *, $p < 0.05$; **, $p < 0.01$; ***, $p < 0.001$, compared with control treatment and analyzed by two-tailed T test. Data are represented as mean ± SEM.

(B) 2D10, J-Lat A1, and U1 cells were treated with 10 nM IAPi, 40 mM NaCr, or their combination for 24 h. Percentage of GFP positive cells in 2D10 and J Lat A1 was analyzed by flow cytometry, whereas HIV RNA in U1 cells was analyzed by qPCR (n = 3). **, $p < 0.01$; ***, $p < 0.001$, analyzed by two-tailed T test. Data are represented as mean ± SEM.

significantly enhance ncNF-κB-induced latency reversal in all models (Figures 1 and 2). We therefore sought to explore the possibility that crotonylation enhanced ncNF-κB signaling and reactivation of latent HIV *via* mechanisms beyond the known effect of crotonylation on histones (Jiang et al., 2018). We treated 2D10 cells with NaCr and a submaximal concentration of AZD5582 (1 nM) individually or with a combination of the two drugs for 24 h. Western blot analysis showed that, in whole cell protein lysates, AZD5582 alone effectively reduced cIAP1 and cIAP2 protein levels, leading to lower p100 level and increased p52 level, indicative of cleavage, without impact on other proteins such components of the elongation complex needed for efficient HIV transcription, p-TEFb, the cNF-κB signaling protein RelA, and the autophagy and cell death proteins LC3B, PARP1, and Caspase 3 (Campbell et al., 2018) (Figure 5B). This differs from a previous report where IAPi alone induced cleavage of Caspase 3 and LC3B, leading to autophagy and/or cell death in memory CD4+ T cells. This may be caused by different responses among cell types studied (Campbell et al., 2018). However, this was consistent with our observations above where no significant cell death was induced by IAPi alone unless in combination with crotonate (Figure 4).

Combination treatment trended toward increased p100 gene expression, although not significantly, compared with LRA treatment alone (Figure S4. [Gene expression of p100 in 2D10 cells model of HIV latency], related to Figure 5). There was no significantly enhanced induction of ACSS2, the enzyme essential for protein crotonylation that plays a direct role in HIV latency reversal (Jiang et al., 2018). This suggested that the synergy observed between AZD8852 and crotonate may not occur solely through direct enhancement of crotonylation activity. As we reported previously in latency models of J-Lat A1 cells and primary CD4+ T cells (Jiang et al., 2018), the addition of crotonate enhanced ACSS2 protein expression in 2D10 cells (Figure 5B). Notably, when AZD5582 and NaCr were administered in combination, the p52 band was greatly enhanced. This suggests an effect of crotonate on the conversion of p100 to p52, enhancing ncNF-kB signaling. A similar enhancement of p52 levels was observed in J-Lat 10.6 and J-Lat A1 cell models of latency where combination treatment of AZD5582 with crotonate enhanced p52 levels (Figure 5C).

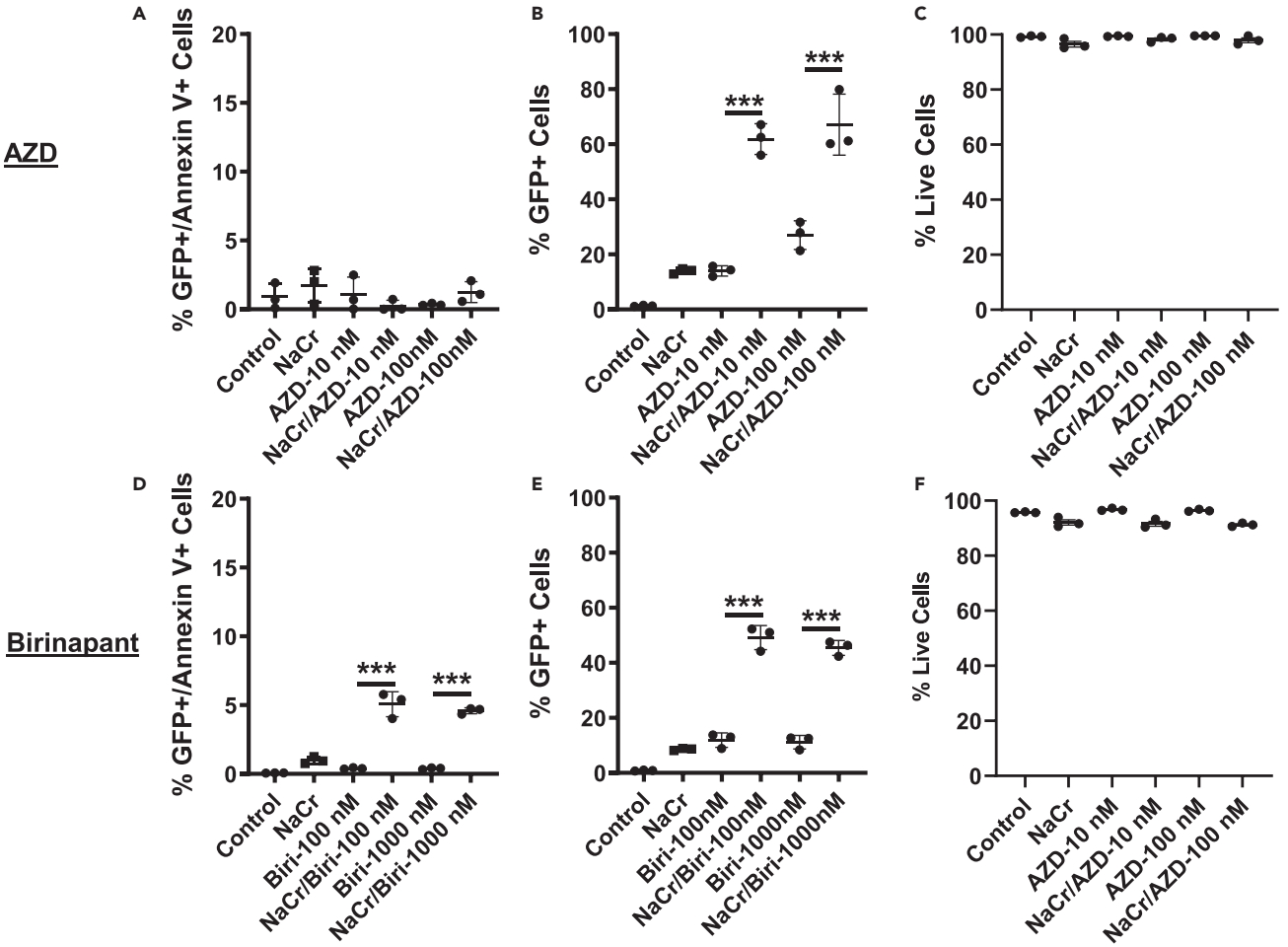

Figure 4. Crotonylation and IAPi treatment induce limited apoptosis while synergistically reactivating HIV in 2D10 cells

(A–C) 2D10 cells were treated with different doses of AZD5582 (AZD), 40 mM NaCr, or in combination for 24 h. Apoptosis (Annexin V) (A), percentage of GFP positive cells (B) and cellular viability (C) were analyzed by flow cytometry where % GFP+/Annexin V+ represented cell death in latency disrupted cells. (D–F) 2D10 cells were treated with different doses of Birinapant, 40 mM NaCr, or in combination for 24 h. Apoptosis, percentage of GFP positive cells and cellular viability were similarly analyzed as in (A–C). ***, $p < 0.001$, analyzed by one-way ANOVA (n = 3). Data are represented as mean ± SEM.

Surprisingly, in U1 cells, no significant enhancement in cleavage of p100 was seen when U1 cells were treated in combination, whereas NaCr alone appeared to induce p100 cleavage (Figure 5C). In the primary CD4+ T cell model of latency, even though the combination treatment reduced p100 protein levels, p52 level was not increased. This could be because of the fact that p52 stability is impaired even when p100 cleavage was enhanced in this primary CD4+ T cell model of latency, which may hamper optimal induction of HIV transcription from latency by IAPi (Figure 5C). To further explore the mechanism as to why combination treatment failed to boost p52 levels even though HIV transcription was enhanced in U1 cells, we assessed whether nuclear p52 was enhanced by crotonylation in U1 cells. When U1 cells were fractionated, no increase of p52 production was observed either in the nucleus or in the cytoplasm after AZD5582/NaCr treatment. In contrast, in 2D10 cells, AZD5582 alone induced p52 production which was further augmented by combination treatment in both the nucleus and cytoplasm (Figure 5D). These data indicate that the response of the promonocytic cell line U1 to crotonate/AZD5582 may differ from CD4+ T cells.

Crotonate sensitizes IAPi-induced ncNF-κB reactivation of resting CD4+ T cells isolated from ART-suppressed individuals *ex vivo*

Although it is difficult to study LRA activity in the resting CD4+ T cells from HIV-infected, ART-treated, and aviremic donors, this is the most relevant system for *ex vivo* validation. Therefore, we tested whether crotonate enhances cell-associated HIV RNA expression in such cells induced by AZD5582 (Table 1, n = 7).

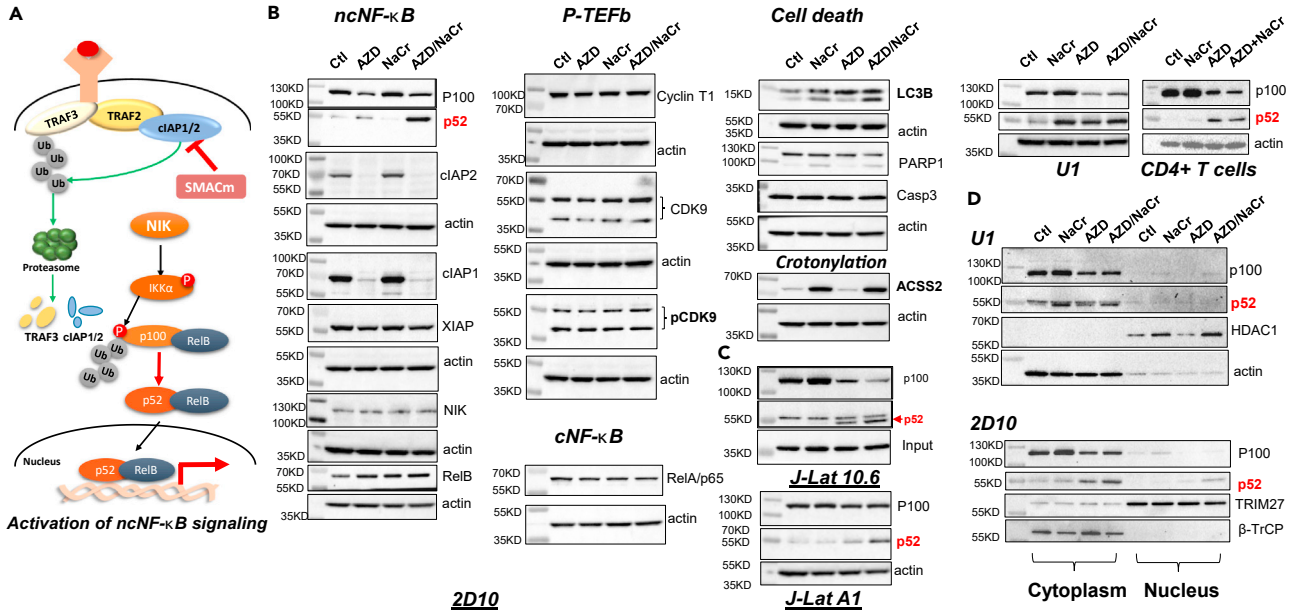

Figure 5. Crotonylation stimulated p100 cleavage into p52 in ncNF-κB pathway in CD4+ T cells

(A) Model of ncNF-kB signaling pathway and the site of action of IAPi/SMACm.

(B) 2D10 cells were treated with 1 nM AZD5582 (AZD), 40 mM NaCr or their combination. Cells were harvested 24 h posttreatment and total proteins were prepared for Western blot.

(C) J-Lat A1 cells were treated with 1 nM AZD, 40 mM NaCr or their combination. U1 cells were treated with 5 nM AZD, or 20 mM NaCr or their combination while J-Lat 10.6 cells were treated with 10 nM AZD, or 40 mM NaCr or their combination. Primary CD4+ T cells were treated with 100 nM AZD, or 30 mM NaCr or their combination. Cells were harvested 24 h posttreatment and total proteins were prepared for the examination of p100/52 protein cleavage by Western blot.

(D) U1 or 2D10 cells were treated as in (C). Then, nucleus and cytoplasm were fractionated and subjected for Western blot analysis, where actin and β-TrCP served as cytoplasmic protein controls and HADC1 or TRIM27 served as nuclear protein controls. Data are represented as mean ± SEM.

Resting CD4+ T cells were treated with 30 mM NaCr, 100 nM AZD5582, or with the combination of 30 mM NaCr and 100 nM AZD5582. The cells were collected 24 and 48 h posttreatment and cell-associated HIV *gag* RNA expression was measured. We found that either the induction of crotonylation by NaCr or the activation of ncNF-κB signaling by IAPi AZD5582 alone was able to disrupt latent HIV in resting CD4+ T cells, which was consistent with our previous observations (Jiang et al., 2018; Nixon et al., 2020). Importantly, the combination of crotonylation induction by NaCr and ncNF-κB activation by AZD5582 enhanced latency reversal, compared to AZD5582 induction alone (*t* test, $p < 0.05$). The induction of cellular toxicity was assessed in primary HIV negative CD4 T cells from additional donors, and was minimal: 5% reduction in viability in AZD5582 alone *vs* 8% in cells with combination treatment where overall apoptosis was <1.6% (Figures 6 and S5. [Cellular viability in primary CD4+ T cell], related to Figure 6). Enhancement of HIV production by combination treatment was more pronounced 24 h posttreatment. Indeed, the fold induction of HIV transcription achieved significant 24 h, but not 48 h, posttreatment compared with AZD5582 treatment alone (Figures 6C and 6D). This *ex vivo* evidence supports the idea that crotonylation induction enhances HIV transcription or latency reversal elicited by IAPi-activated ncNF-κB signaling.

LC MS/MS and GO enrichment analysis of protein crotonylome in latent and reactivated cells

To understand how protein crotonylation enhances ncNF-kB signaling, we performed a quantitative proteomic analysis of proteins isolated by anti-pan-crotonyl-Lysine antibodies from whole 2D10 cell lysates. Cells were untreated or treated with crotonate for 6 h (Figures 7A–7C). We reasoned that a shorter exposure of crotonate to cells will reduce the indirect and secondary impact triggered by crotonate-induced cellular metabolism. A total of 339 proteins were identified, among them 258 proteins were characterized with more than two unique peptides. In control and NaCr-treated cells, 45 proteins were differentially immunoprecipitated (Figure 7D); 6 proteins were isolated from untreated cells and 39 proteins were from NaCr-treated cells. Overall, 19 crotonylated proteins were identified, which contained 26 direct

Table 1. Participant information in this study

Study PID	Years on ART	Years suppressed	CD4 T count (cells/μl)	Age	Sex[a]	Race[b]	ART regimen	Treatment Status[c]
Pt 1	8.2	7	642	32	M	AA	Atripla (EFV/FTC/TDF)	CHI
Pt 2	8.4	2.2	631	52	M	W	Biktarvy (BIC/FTC/TAF)	CHI
Pt 3	20.5	5.2	928	41	M	AA	Biktarvy (BIC/FTC/TAF)	CHI
Pt 4	8.7	7.8	372	48	M	W	Biktarvy (BIC/FTC/TAF)	CHI
Pt 5	11.6	6.3	788	42	M	H	Descovy/Tivicay (FTC/TAF/DAG)	CHI
Pt 6	33.9	11.2	669	59	M	W	Atripla (EFV/FTC/TDF)	CHI
Pt 7	4.6	4.3	936	27	M	W	Genvoya (EVG/COBI/FTC/TAF)	CHI

[a]M, male.
[b]AA, African American; W, White; H, Hispanic.
[c]CHI, chronic HIV infection.

crotonylation sites. GO Enrichment analysis indicated that, in NaCr-treated cells, almost all proteins were involved in gene transcription and posttranscriptional regulation, such as mRNA processing, splicing, and maturation (Figure S6 [Pathway analysis of crotonylome], related to Figure 7). Differentially immunoprecipitated proteins in untreated cells compared to NaCr-treated cells were related to the TCA cycle and acyl-CoA metabolism, apart from one protein, TRIM27. Although not directly crotonylated, TRIM27, an E3 ubiquitin ligase, was of special interest as the ubiquitination pathway is essential for the cleavage of p100 into p52 in the ncNF-kB pathway.

TRIM27 siRNA knockdown decreases HIV transcription at the step of p100/p52 cleavage

It has been reported that TRIM27, an E3 ubiquitin ligase, is involved in viral replication, alone or with its deubiquitination partner protein USP7 (Zheng et al., 2019). For example, TRIM27 upregulates replication of HCV by suppressing type I interferon response (Zheng et al., 2019). In contrast, when complexed with USP7, TRIM27 can also act as a negative regulator in antiviral signaling (Cai et al., 2018; Hao et al., 2015). To investigate the role of TRIM27 in the regulation of ncNF-κB signaling during latency reversal, TRIM27 was depleted in 2D10 cells using specific siRNAs (Figures 8A and 8B) (Bronevetsky et al., 2016). This caused a significant reduction in the latency reversal induced by the ncNF-κB inducer AZD5582 (Figure 8C). Notably, following IAPi exposure, both p100 and p52 were absent in the TRIM27 siRNA condition (Figure 8B) without significant impact in p100 gene expression (Figure S7. [The impact of TRIM27 siRNA knockdown in p100 gene expression], related to Figure 8). Interestingly, in the basal condition (absence of IAPi treatment), knockdown of TRIM27 slightly reduced p100 levels without impact in the production of p52 (Figure S7. [The impact of TRIM27 siRNA knockdown in p100 gene expression], related to Figure 8), indicating that TRIM27 may largely affect ncNF-κB p100/p52 cleavage machinery when it has been assembled and activated. Knockdown TRIM27 in the primary CD4+ T cell model of latency also reduced p100/p52 protein levels and significantly dampened NaCr-induced HIV latency reversal (Figures 8D–8F), indicating that TRIM27 is involved in the ncNF-κB-dependent HIV transcription. Taken together, these data suggest that TRIM27 may play a role in ncNF-κB signaling through the regulation of p100/p52 cleavage step.

TRIM27 and USP7 physically and functionally interact with each other in T cells

The interaction of TRIM27 with the deubiquitinase USP7 maintains TRIM27 stability and its E3 ligase activity (Cai et al., 2018). To study this system in the context of HIV latency reversal, we performed a co-immunoprecipitation analysis with the whole cell protein lysate from 2D10 cells. Cells were treated with AZD5582, NaCr along or with the combination of the two compounds for 24 h. Our data showed that TRIM27 immunoprecipitated with USP7, indicating that they are in the same complex, consistent with reports in other systems (Hao et al., 2015) (Figure 9A). Small molecules to directly inhibit USP7 deubiquitinases are under development as a pharmacologic intervention in many diseases (Li and Liu, 2020). To test whether USP7/TRIM27 complex functionally affects HIV latency reversal, 2D10 cells were treated with the USP7 deubiquitinase inhibitor (USP7i) P5091, which suppresses USP7 deubiquitinase activity, and therefore should destabilize the TRIM27 protein. We found that USP7i potently suppressed the induction of HIV by the combination of NaCr and AZD5582 (Figure 9B). When further analyzed by Western blot, we found that the inhibition of USP7 by P5091 in AZD/NaCr-treated cells partially reduced TRIM27 protein. Surprisingly, NaCr seemed to slightly enhance TRIM27 protein levels. However, the underlying mechanism is not clear and

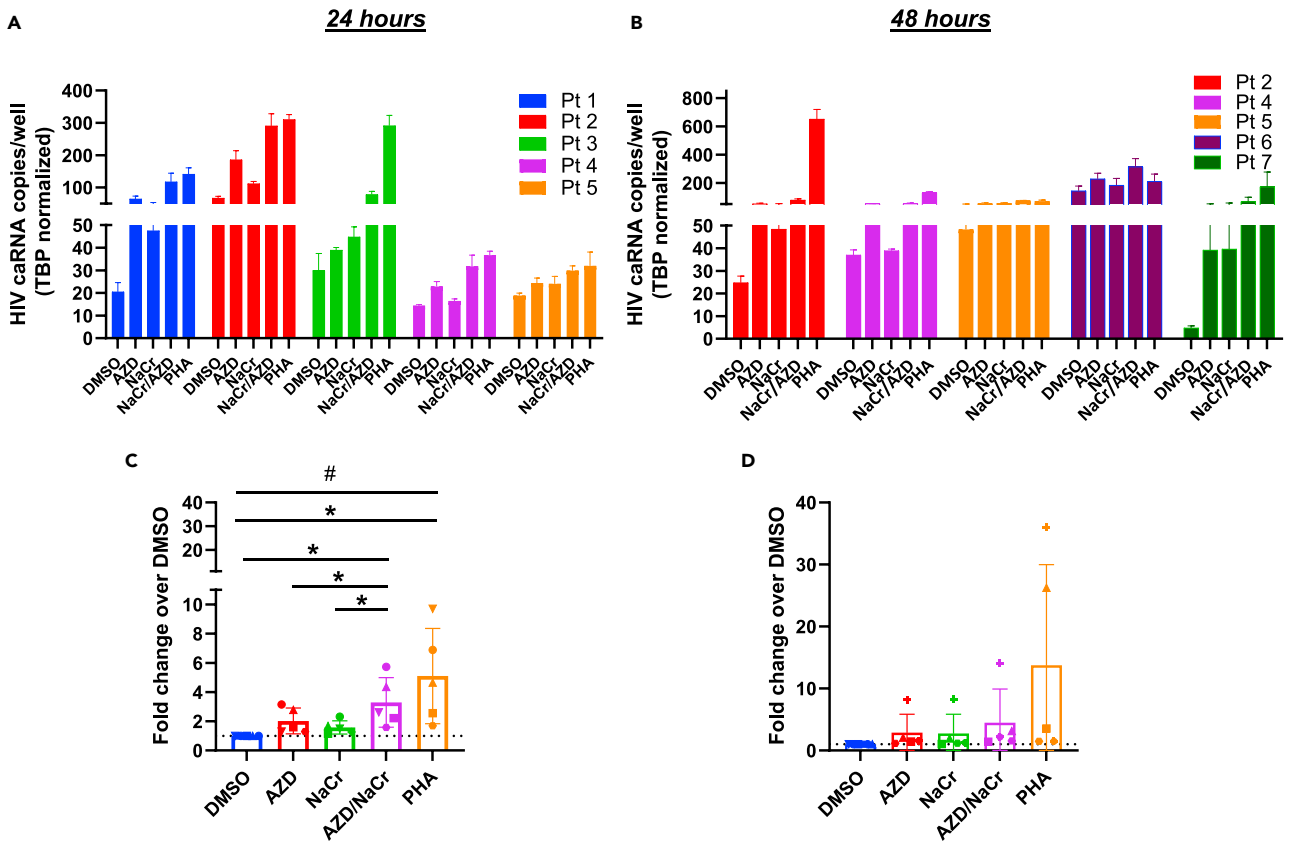

Figure 6. Crotonylation enhances AZD5582-induced latency reversal in resting CD4+ T cells isolated from HIV + individuals receiving ART

(A and B) Resting CD4+ T cells from HIV + individuals durably suppressed on ART were treated with 100 nM AZD5582 (AZD), 30 mM NaCr, phytohemagglutinin (PHA, T cell mitogen to induce immune activation), and IL-2 or in combination for 24 h (n = 5, (A) or 48 h (n = 5, (B). Cells were harvested and HIV *gag* RNA copies were analyzed using 3–5 replicate RNA extractions from 2-4 million cells per replicate for each condition with normalization to the reference gene TBP, with the exception of PHA/IL-2 because of the known upregulation of TBP by prolonged mitogen exposure.

(C and D) The above data was analyzed with fold change of HIV expression was analyzed after HIV copies normalized to DMSO control treatment. *, $p < 0.05$ by two-tailed T test. #, $p < 0.05$ by One-way ANOVA. Data are represented as mean ± SEM. Each symbol represents the average fold induction for a separate donor.

warrants further investigation because it may be related to crotonylation function. Similar to the impact of TRIM27 siRNA knockdown (Figure 8C), USP7i also reduced both p100 and p52 protein levels (Figure 9C), leading to the reduced latency reversal. These observations further suggest that TRIM27, in the complex with USP7, contributes to HIV transcription by enhancing AZD5582-induced p100 cleavage into p52 possibly *via* stabilizing both p100 and p52 proteins, thereby stimulating ncNF-κB signaling to disrupt latent HIV.

DISCUSSION

A major obstacle for the clearance of HIV infection, cellular reservoirs of latent virus, cannot be purged by current ART (Archin et al., 2014; Margolis et al., 2020; Sengupta and Siliciano, 2018). Studies in the last decades have expanded our understanding of how HIV latency is established (Jiang and Dandekar, 2015; Margolis et al., 2020; Sengupta and Siliciano, 2018). Strategies to purge the HIV reservoir have been proposed and are being tested in preclinical and clinical studies (Archin et al., 2014; Margolis et al., 2020; Sengupta and Siliciano, 2018). It has become clear that HIV latency is controlled by multiple layers of regulation (Archin et al., 2014; Cary et al., 2016; Jiang and Dandekar, 2015; Margolis et al., 2020; Sengupta and Siliciano, 2018), and that strategies that target a single mechanism of latency regulation thus far cannot broadly or potently disrupt latent HIV across infected cell populations, and may fail to induce sufficient viral antigen to allow for immune clearance.

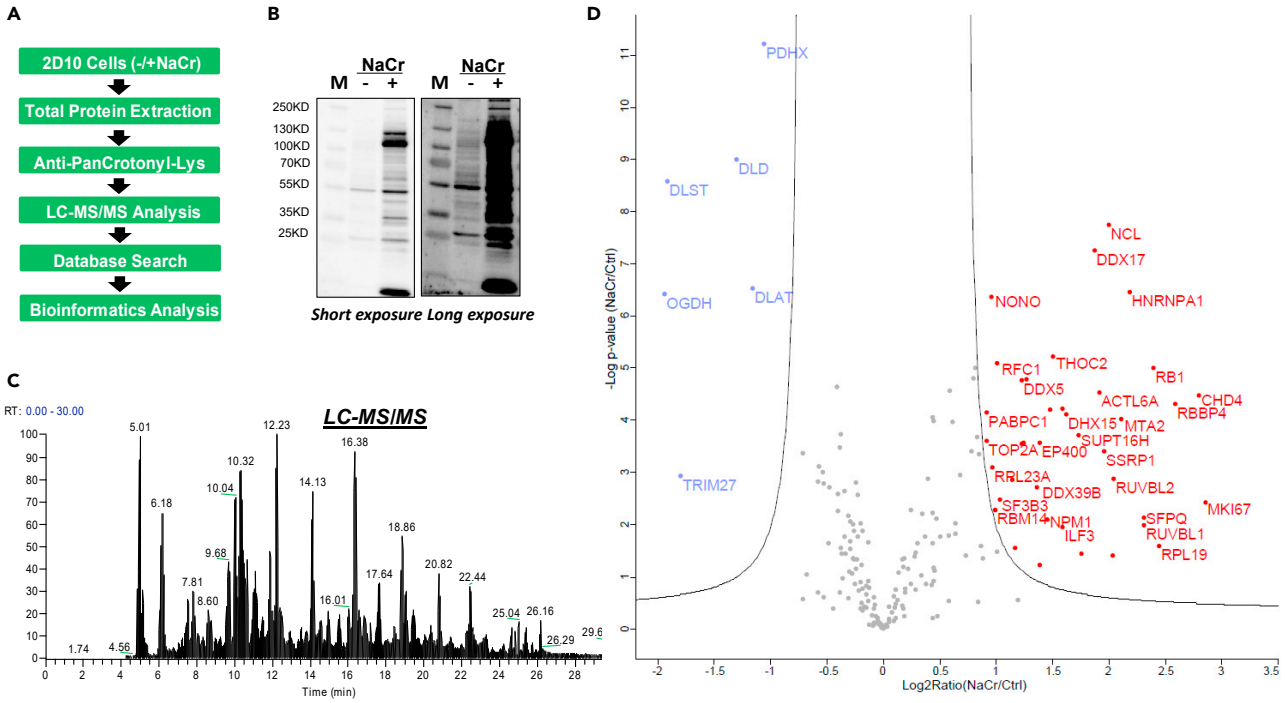

Figure 7. Quantitative Mass-Spec analysis of crotonylation proteome

2D10 cells were treated with or without 30 mM NaCr for 6 h (n = 3). Cells were harvested for immunoprecipitation by anti-Pancrotonyl-Lysine antibody. Immunoprecipitated proteins were analyzed by quantitative mass spectrometry

(A) Schematic diagram of the experimental design for comprehensive identification of immunoprecipitated proteins.

(B) Western blot showed crotonylated protein in the latent and NaCr-reactivated 2D10 cells where M refers to the protein marker.

(C) Representative total ion chromatogram of tryptic peptides in the immunoprecipitated protein.

(D) Volcano plot showed 45 differentially expressed proteins in latent cells vs NaCr-reactivated cells.

In this report, we found that crotonylation enhances IAPi-induced ncNF-κB signaling to disrupt HIV latency. In addition to the known effects of crotonylation on histones at the HIV LTR, enhanced processing of p100 to p52 in the ncNF-kB pathway is mediated by crotonylation, and/or a downstream effect of crotonylation, leading to synergistic HIV LTR induction. Quantitative proteomic analyses and biochemical assays suggest that the E3 ubiquitination ligase TRIM27 may be involved in this enhancement at the p100 cleavage step. As the induction of ncNF-κB signaling shows promise in reactivating latent HIV *in vivo* (Nixon et al., 2020), the strategy to enhance ncNF-κB-mediated latency reversal by crotonylation provides an additional tool for a robust disruption of latent HIV for HIV cure. This warrants further investigation in the future.

It is interesting that the activity of IAPi may also be related to cell type as the promonocytic U1 cell model of latency appears to be less sensitive to IAPi, even at high concentrations (Figures 3 and 5). Other approaches may be required to effectively reverse latency in this model. However, crotonate alone induced an unexpectedly efficient cleavage of p100 into p52 in the U1 model of latency. These observations suggest that ncNF-κB signaling may regulate HIV transcription differently across cell types, whereas crotonylation seems to be involved in ncNF-κB activation in U1 cells. Even though IAPi alone was unable to effectively induce HIV transcription in U1 cells, latent HIV can be disrupted when in combination with crotonylation (Figure 3). This supports the concept that the combination of crotonylation with ncNF-κB induction may be advantageous in latency reversal (Figure 3C).

IAPis also have the potential to induce apoptosis of HIV-infected cells. In both Jurkat and primary CD4+ T cell models of latency, we were unable to see a significant apoptosis induction by IAPi treatment alone, despite effective latency reversal. This differed from previous observations (Campbell et al., 2018), perhaps because of the cell models studied. Interestingly, crotonylation in combination with Birinapant, but not in combination with AZD5582, induced a modest degree of cell death in cells that also expressed HIV

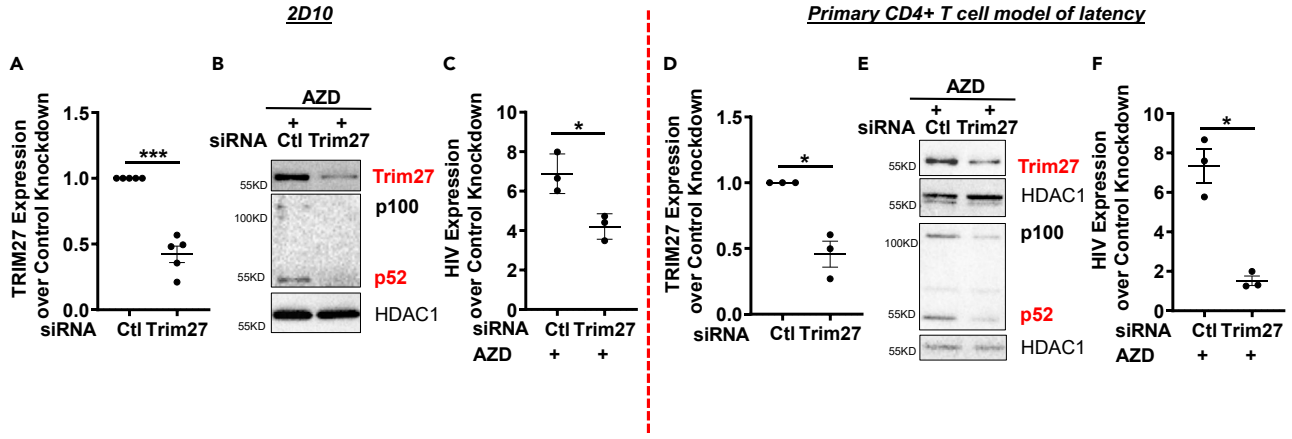

Figure 8. TRIM27 is involved in HIV transcription

(A–C) TRIM27 was knocked down in 2D10 cells after transfection of control siRNA or TRIM27 siRNA. Two days after knockdown, the cells were treated with AZD5582 (AZD) overnight. Then, the cells were harvested and TRIM27 and HIV RNA expression was analyzed by qPCR. *, $p < 0.05$; ***, $p < 0.001$, analyzed by two-tailed T test (n = 3–5). Data are represented as mean ± SEM.

(D–F) TRIM27 was knocked down in the primary CD4+ T cell model of latency after transfection of control siRNA or TRIM27 siRNA. Two days after knockdown, the cells were treated with AZD5582 (AZD) overnight. Then, the cells were harvested and TRIM27 and HIV RNA expression was analyzed by qPCR (F). *, $p < 0.05$, analyzed by two-tailed T test (n = 3). Data are represented as mean ± SEM.

LTR-driven genes in the Jurkat model of latency (Figure 4), indicating that directly inducing cell death by IAPi is achievable but complex and incompletely understood.

The discovery of TRIM27 as a potential candidate participating in ncNF-κB activation is unexpected. This was supported by the observations that knockdown of TRIM27 reduced HIV transcription and impaired the production of p100/p52 (Figure 8). However, TRIM27 knockdown did not completely dampen AZD5582-induced latency reversal, this may be because of the incomplete TRIM27 knockdown or small molecule AZD5582 may trigger other signaling pathways related to HIV transcription, but currently not discovered. Considering that TRIM27 is primarily a nuclear protein (Figure 5D), TRIM27 may be particularly involved in stabilizing p52 in the nucleus. Interestingly, TRIM27 is often complexed with the deubiquitinase protein USP7 (Cai et al., 2018). This maintains TRIM27 E3 ligase activity by suppression of TRIM27 auto-ubiquitination. However, it is unclear whether this is involved in the transcription of HIV in CD4+ T cells during its regulation of ncNF-κB signaling. Nevertheless, inhibition of USP7 by its pharmacologic inhibitor P5091 abrogated NaCr/AZD-induced latency disruption and impaired p52 stability. This supports the hypothesis that TRIM27, in the complex with USP7, regulates HIV transcription (Figures 9B and 9C). Whether protein crotonylation is directly involved in TRIM27-associated ncNF-κB signaling remains to be determined. Considering that TRIM27 is an E3 ligase, how knockdown of TRIM27 impaired p52 stability (or p100) is not understood. Crotonylation and/or TRIM27 may further regulate the well-described p100 processing *via* the SCF ubiquitin ligase β-TRCP complex. Inhibition of USP7 is under development as a pharmaceutic target for cancer therapy (Li and Liu, 2020). It is possible that USP7 can be further exploited as part of the "lock and block" strategy for HIV cure by impairment of the function of TRIM27 and inhibition of ncNF-κB signaling to enforce latency.

Taken together, we find that crotonate enhances IAPi-induced ncNF-κB signaling to disrupt latency. This was possibly controlled by TRIM27 ubiquitination signaling pathway at the step of p100 cleavage into p52, in addition to the epigenetic regulation of HIV transcription at the HIV LTR (Jiang et al., 2018). These findings provide a deep understanding of the complexity of NF-κB signaling during HIV transcription and the establishment of HIV latency (Wong and Jiang, 2021; Yang et al., 2020), which will help us design alternative tools to deplete stable HIV reservoirs in future.

Limitations of the study

In this study, we have tested several models of HIV latency, including Jurkat models, primary CD4+ T cell models and resting CD4+ T cells isolated from ART-suppressed PLWH, to study the impact of crotonylation

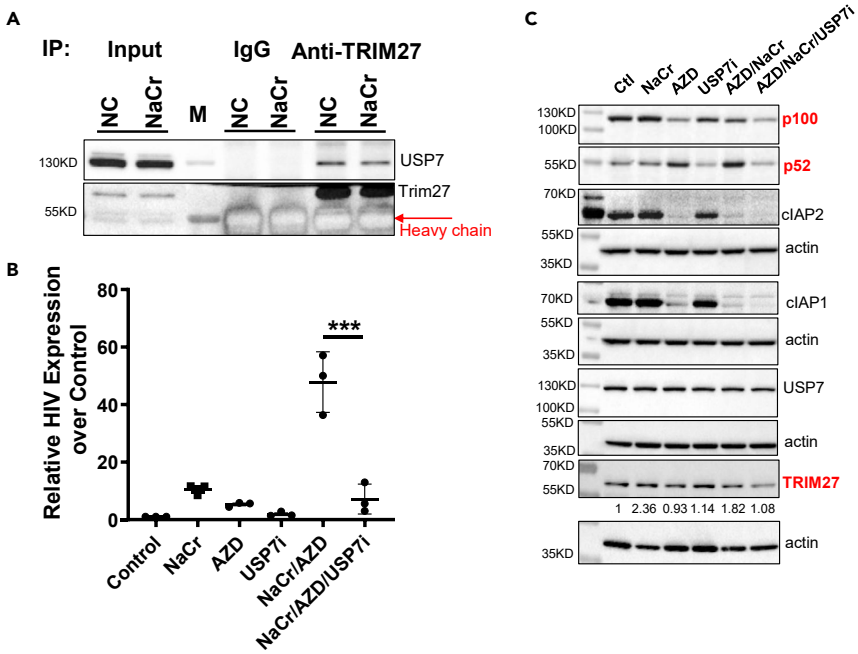

Figure 9. TRIM27 interacts with USP7 to upregulate HIV transcription

(A) 2D10 cells were treated with or without 40 mM NaCr for 24 h. Cells were harvested for immunoprecipitation by anti-TRIM27 antibody, followed by Western blot with anti-TRIM27 antibody and anti-USP7 antibody.

(B) 2D10 cells were treated with 1 nM AZD5582 (AZD), 30 mM NaCr, 5 μM USP7 inhibitor (USP7i) P5091 or their combinations for 24 h. Cells were harvested and total RNA were isolated for HIV RNA expression analyses by qPCR (n = 3). ***, $p < 0.001$, analyzed by One-way ANOVA test. Data are represented as mean ± SEM.

(C) 2D10 cells were treated as in B and total proteins were prepared to examine ncNF-κB related protein expression.

in the enhancement of AZD5582-induced latency reversal and the activation of ncNF-κB signaling. Although in general crotonate enhanced AZD5582-induced latency reversal, no enhancement was observed in U1 cells. In fact, crotonate alone induced high levels of p52, indicating that crotonylation may be indirectly involved in ncNF-κB activation. However, this was not tested in the other macrophage model of latency, because of the lack of appropriate macrophage-derived latent models. In the primary CD4+ T cell models, we also observed some different degrees of latency enhancement induced by crotonate when different sources of donors were used. This was highlighted by the decreased p100 levels but no enhancement of p52 (Figure 4C), indicating that although crotonylation slightly induces p100 cleavage, p52 is not stable enough to further boost latency reversal. It may be important to stabilize p52 in order to achieve a robust HIV transcription from latency in primary CD4 T cells. In addition, latency reversal might be further improved when the cells are treated longer with IAPi and NaCr or with IAPi because it is well-known that ncNF-κB signaling is slow but persistent compared with cNF-κB activation (Sun, 2012, 2017). These interesting and important observations further highlight the complexity of HIV transcription machinery and HIV latency, which provide us useful information to deepen our understanding of HIV latency and the cure of HIV in future.

STAR★METHODS

Detailed methods are provided in the online version of this paper and include the following:

- KEY RESOURCES TABLE
- RESOURCE AVAILABILITY
  - Lead contact
  - Materials availability
  - Data and code availability
- EXPERIMENTAL MODEL AND SUBJECT DETAILS
  - Cell models

SUPPLEMENTAL INFORMATION

Supplemental information can be found online at https://doi.org/10.1016/j.isci.2021.103649.

ACKNOWLEDGMENTS

We thank Dr. Richard Dunham for his critical reading and insightful suggestions and Dr. Jonathan Karn for his 2D10 model of latency. We also thank the participants who donated samples for this study. This work was supported by Qura Therapeutics (2019-01) to GJ, NIH 1R01AI143381-01A1 to EPB, NIH R01 GM133107-01 and R21 AG071229-01 to XC, and Delaney Collaboratory for AIDS Eradication (CARE) UM1AI126619 to DMM.

AUTHOR CONTRIBUTIONS

GJ conceived the study. DL, LMW, YT performed the experiments in latency models *in vitro and ex vivo*. MGD, SDF, and NMA performed latency reversal analysis in resting CD4+ T cells isolated from PLWH *ex vivo*. LW and XC performed proteomic analysis. EPB established a primary CD4+ T cell model of latency. DMM provided scientific advice. DJ and GJ assembled the data and wrote the manuscript. All authors read and revised multiple versions of initial writing and approved the manuscript.

DECLARATION OF INTERESTS

GJ has a related patent application (Publication number: 20,200,268,856). Other authors declare no conflict of interest.

Received: July 19, 2021
Revised: November 8, 2021
Accepted: December 15, 2021
Published: January 21, 2022

REFERENCES

Archin, N.M., Liberty, A.L., Kashuba, A.D., Choudhary, S.K., Kuruc, J.D., Crooks, A.M., Parker, D.C., Anderson, E.M., Kearney, M.F., Strain, M.C., et al. (2012). Administration of vorinostat disrupts HIV-1 latency in patients on antiretroviral therapy. Nature *487*, 482–485.

Archin, N.M., Sung, J.M., Garrido, C., Soriano-Sarabia, N., and Margolis, D.M. (2014). Eradicating HIV-1 infection: seeking to clear a persistent pathogen. Nat. Rev. Microbiol. *12*, 750–764.

Banerjee, C., Archin, N., Michaels, D., Belkina, A.C., Denis, G.V., Bradner, J., Sebastiani, P., Margolis, D.M., and Montano, M. (2012). BET bromodomain inhibition as a novel strategy for reactivation of HIV-1. J. Leukoc. Biol. *92*, 1147–1154.

Bradley, T., Ferrari, G., Haynes, B.F., Margolis, D.M., and Browne, E.P. (2018). Single-cell analysis of quiescent HIV infection reveals host transcriptional Profiles that regulate proviral latency. Cell Rep. *25*, 107–117.e3.

Bronevetsky, Y., Burt, T.D., and McCune, J.M. (2016). Lin28b regulates fetal regulatory T cell differentiation through modulation of TGF-beta signaling. J. Immunol. *197*, 4344–4350.

Cai, J., Chen, H.Y., Peng, S.J., Meng, J.L., Wang, Y., Zhou, Y., Qian, X.P., Sun, X.Y., Pang, X.W., Zhang, Y., et al. (2018). USP7-TRIM27 axis negatively modulates antiviral type I IFN signaling. FASEB J. *32*, 5238–5249.

Campbell, G.R., Bruckman, R.S., Chu, Y.L., Trout, R.N., and Spector, S.A. (2018). SMAC mimetics induce autophagy-dependent apoptosis of HIV-1-Infected resting memory CD4+ T cells. Cell Host Microbe *24*, 689–702 e687.

Cary, D.C., Fujinaga, K., and Peterlin, B.M. (2016). Molecular mechanisms of HIV latency. J. Clin. Invest. *126*, 448–454.

Chun, T.W., Stuyver, L., Mizell, S.B., Ehler, L.A., Mican, J.A., Baseler, M., Lloyd, A.L., Nowak, M.A., and Fauci, A.S. (1997). Presence of an inducible HIV-1 latent reservoir during highly active antiretroviral therapy. Proc. Natl. Acad. Sci. U S A *94*, 13193–13197.

Condon, S.M., Mitsuuchi, Y., Deng, Y., LaPorte, M.G., Rippin, S.R., Haimowitz, T., Alexander, M.D., Kumar, P.T., Hendi, M.S., Lee, Y.H., et al. (2014). Birinapant, a smac-mimetic with improved tolerability for the treatment of solid tumors and hematological malignancies. J. Med. Chem. *57*, 3666–3677.

Darcis, G., Kula, A., Bouchat, S., Fujinaga, K., Corazza, F., Ait-Ammar, A., Delacourt, N., Melard, A., Kabeya, K., Vanhulle, C., et al. (2015).

An in-depth comparison of latency-reversing agent combinations in various in vitro and ex vivo HIV-1 latency models identified bryostatin-1+JQ1 and ingenol-B+JQ1 to potently reactivate viral gene expression. PLoS Pathog. *11*, e1005063.

Finzi, D., Hermankova, M., Pierson, T., Carruth, L.M., Buck, C., Chaisson, R.E., Quinn, T.C., Chadwick, K., Margolick, J., Brookmeyer, R., et al. (1997). Identification of a reservoir for HIV-1 in patients on highly active antiretroviral therapy. Science *278*, 1295–1300.

Friedman, J., Cho, W.K., Chu, C.K., Keedy, K.S., Archin, N.M., Margolis, D.M., and Karn, J. (2011). Epigenetic silencing of HIV-1 by the histone H3 lysine 27 methyltransferase enhancer of Zeste 2. J. Virol. *85*, 9078–9089.

Gay, C.L., Kuruc, J.D., Falcinelli, S.D., Warren, J.A., Reifeis, S.A., Kirchherr, J.L., James, K.S., Dewey, M.G., Helms, A., Allard, B., et al. (2020). Assessing the impact of AGS-004, a dendritic cell-based immunotherapy, and vorinostat on persistent HIV-1 Infection. Sci. Rep. *10*, 5134.

Gutierrez, C., Serrano-Villar, S., Madrid-Elena, N., Perez-Elias, M.J., Martin, M.E., Barbas, C., Ruiperez, J., Munoz, E., Munoz-Fernandez, M.A., Castor, T., et al. (2016). Bryostatin-1 for latent virus reactivation in HIV-infected patients on antiretroviral therapy. AIDS *30*, 1385–1392.

Hao, Y.H., Fountain, M.D., Jr., Fon Tacer, K., Xia, F., Bi, W., Kang, S.H., Patel, A., Rosenfeld, J.A., Le Caignec, C., Isidor, B., et al. (2015). USP7 acts as a molecular rheostat to promote WASH-dependent endosomal protein recycling and is mutated in a human neurodevelopmental disorder. Mol. Cell *59*, 956–969.

Hennessy, E.J., Adam, A., Aquila, B.M., Castriotta, L.M., Cook, D., Hattersley, M., Hird, A.W., Huntington, C., Kamhi, V.M., Laing, N.M., et al. (2013). Discovery of a novel class of dimeric Smac mimetics as potent IAP antagonists resulting in a clinical candidate for the treatment of cancer (AZD5582). J. Med. Chem. *56*, 9897–9919.

Jiang, G., and Dandekar, S. (2015). Targeting NF-kappaB signaling with protein kinase C agonists as an emerging strategy for combating HIV latency. AIDS Res. Hum. Retrovir. *31*, 4–12.

Jiang, G., Espeseth, A., Hazuda, D.J., and Margolis, D.M. (2007). c-Myc and Sp1 contribute to proviral latency by recruiting histone deacetylase 1 to the human immunodeficiency virus type 1 promoter. J. Virol. *81*, 10914–10923.

Jiang, G., Mendes, E.A., Kaiser, P., Sankaran-Walters, S., Tang, Y., Weber, M.G., Melcher, G.P., Thompson, G.R., 3rd, Tanuri, A., Pianowski, L.F., et al. (2014). Reactivation of HIV latency by a newly modified Ingenol derivative via protein kinase Cdelta-NF-kappaB signaling. AIDS *28*, 1555–1566.

Jiang, G., Mendes, E.A., Kaiser, P., Wong, D.P., Tang, Y., Cai, I., Fenton, A., Melcher, G.P., Hildreth, J.E., Thompson, G.R., et al. (2015). Synergistic reactivation of latent HIV expression by ingenol-3-angelate, PEP005, targeted NF-kB signaling in combination with JQ1 induced p-TEFb activation. PLoS Pathog. *11*, e1005066.

Jiang, G., Nguyen, D., Archin, N.M., Yukl, S.A., Mendez-Lagares, G., Tang, Y., Elsheikh, M.M., Thompson, G.R., 3rd, Hartigan-O'Connor, D.J., Margolis, D.M., et al. (2018). HIV latency is reversed by ACSS2-driven histone crotonylation. J. Clin. Invest. *128*, 1190–1198.

Jiang, G., Maverakis, E., Cheng, M.Y., Elsheikh, M.M., Deleage, C., Mendez-Lagares, G., Shimoda, M., Yukl, S.A., Hartigan-O'Connor, D.J., Thompson, G.R., 3rd, et al. (2019). Disruption of latent HIV in vivo during the clearance of actinic keratosis by ingenol mebutate. JCI Insight *4*, e126027.

Karn, J. (2011). The molecular biology of HIV latency: breaking and restoring the Tat-dependent transcriptional circuit. Curr. Opin. HIV AIDS *6*, 4–11.

Karn, J., and Stoltzfus, C.M. (2012). Transcriptional and posttranscriptional regulation of HIV-1 gene expression. Cold Spring Harb. Perspect. Med. *2*, a006916.

Kessing, C.F., Nixon, C.C., Li, C., Tsai, P., Takata, H., Mousseau, G., Ho, P.T., Honeycutt, J.B., Fallahi, M., Trautmann, L., et al. (2017). In vivo suppression of HIV rebound by didehydro-cortistatin A, a "Block-and-Lock" strategy for HIV-1 treatment. Cell Rep. *21*, 600–611.

Laird, G.M., Bullen, C.K., Rosenbloom, D.I., Martin, A.R., Hill, A.L., Durand, C.M., Siliciano, J.D., and Siliciano, R.F. (2015). Ex vivo analysis identifies effective HIV-1 latency-reversing drug combinations. J. Clin. Invest. *125*, 1901–1912.

Li, P., and Liu, H.M. (2020). Recent advances in the development of ubiquitin-specific-processing protease 7 (USP7) inhibitors. Eur. J. Med. Chem. *191*, 112107.

Li, D.J., Verma, D., and Swaminathan, S. (2012). Binding of cellular export factor REF/Aly by Kaposi's sarcoma-associated herpesvirus (KSHV) ORF57 protein is not required for efficient KSHV lytic replication. J. Virol. *86*, 9866–9874.

Margolis, D.M., Archin, N.M., Cohen, M.S., Eron, J.J., Ferrari, G., Garcia, J.V., Gay, C.L., Goonetilleke, N., Joseph, S.B., Swanstrom, R., et al. (2020). Curing HIV: seeking to target and clear persistent infection. Cell *181*, 189–206.

Marsden, M.D., Loy, B.A., Wu, X., Ramirez, C.M., Schrier, A.J., Murray, D., Shimizu, A., Ryckbosch, S.M., Near, K.E., Chun, T.W., et al. (2017). In vivo activation of latent HIV with a synthetic bryostatin analog effects both latent cell "kick" and "kill" in strategy for virus eradication. PLoS Pathog. *13*, e1006575.

Nixon, C.C., Mavigner, M., Sampey, G.C., Brooks, A.D., Spagnuolo, R.A., Irlbeck, D.M., Mattingly, C., Ho, P.T., Schoof, N., Cammon, C.G., et al. (2020). Systemic HIV and SIV latency reversal via non-canonical NF-kappaB signalling in vivo. Nature *578*, 160–165.

Pache, L., Dutra, M.S., Spivak, A.M., Marlett, J.M., Murry, J.P., Hwang, Y., Maestre, A.M., Manganaro, L., Vamos, M., Teriete, P., et al. (2015). BIRC2/cIAP1 is a negative regulator of HIV-1 transcription and can Be targeted by smac mimetics to promote reversal of viral latency. Cell Host Microbe *18*, 345–353.

Pearson, R., Kim, Y.K., Hokello, J., Lassen, K., Friedman, J., Tyagi, M., and Karn, J. (2008). Epigenetic silencing of human immunodeficiency virus (HIV) transcription by formation of restrictive chromatin structures at the viral long terminal repeat drives the progressive entry of HIV into latency. J. Virol. *82*, 12291–12303.

Sengupta, S., and Siliciano, R.F. (2018). Targeting the latent reservoir for HIV-1. Immunity *48*, 872–895.

Sloane, J.L., Benner, N.L., Keenan, K.N., Zang, X., Soliman, M.S.A., Wu, X., Dimapasoc, M., Chun, T.W., Marsden, M.D., Zack, J.A., et al. (2020). Prodrugs of PKC modulators show enhanced HIV latency reversal and an expanded therapeutic window. Proc. Natl. Acad. Sci. U S A *117*, 10688–10698.

Spina, C.A., Anderson, J., Archin, N.M., Bosque, A., Chan, J., Famiglietti, M., Greene, W.C., Kashuba, A., Lewin, S.R., Margolis, D.M., et al. (2013). An in-depth comparison of latent HIV-1 reactivation in multiple cell model systems and resting CD4+ T cells from aviremic patients. PLoS Pathog. *9*, e1003834.

Sun, S.C. (2012). The noncanonical NF-kappaB pathway. Immunol. Rev. *246*, 125–140.

Sun, S.C. (2017). The non-canonical NF-kappaB pathway in immunity and inflammation. Nat. Rev. Immunol. *17*, 545–558.

Sun, S.C., and Ley, S.C. (2008). New insights into NF-kappaB regulation and function. Trends Immunol. *29*, 469–478.

Wong, L.M., and Jiang, G. (2021). NF-kappaB sub-pathways and HIV cure: a revisit. EBioMedicine *63*, 103159.

Wong, J.K., Hezareh, M., Gunthard, H.F., Havlir, D.V., Ignacio, C.C., Spina, C.A., and Richman, D.D. (1997). Recovery of replication-competent HIV despite prolonged suppression of plasma viremia. Science *278*, 1291–1295.

Yang, X., Wang, Y., Lu, P., Shen, Y., Zhao, X., Zhu, Y., Jiang, Z., Yang, H., Pan, H., Zhao, L., et al. (2020). PEBP1 suppresses HIV transcription and induces latency by inactivating MAPK/NF-kappaB signaling. EMBO Rep. *21*, e49305.

Yukl, S.A., Kaiser, P., Kim, P., Telwatte, S., Joshi, S.K., Vu, M., Lampiris, H., and Wong, J.K. (2018). HIV latency in isolated patient CD4+ T cells may be due to blocks in HIV transcriptional elongation, completion, and splicing. Sci Transl Med *10*, eaap9927.

Zheng, F., Xu, N., and Zhang, Y. (2019). TRIM27 Promotes hepatitis C virus replication by suppressing type I interferon response. Inflammation *42*, 1317–1325.

STAR★METHODS

KEY RESOURCES TABLE

REAGENT or RESOURCE	SOURCE	IDENTIFIER
Antibodies		
anti-cIAP1	abcam	Cat#ab108361
anti-cIAP2	abcam	Cat#ab23423
anti-USP7	Bethyl	Cat#A700-072
anti-p100/52	Cell signaling	Cat#3017
anti-XIAP	Cell signaling	Cat#14334
anti-NF-κB/p65	Cell signaling	Cat#4764
anti-NIK	Cell signaling	Cat#4994
anti-CDK9	Cell signaling	Cat#2316
anti-pCDK9 (Thr186)	Cell signaling	Cat#2549
anti-PARP1	Cell signaling	Cat#9542
anti-Cyclin T1	Cell signaling	Cat#3017
anti-RelB	Cell signaling	Cat#10544
anti-AceS1 (ACSS2)	Cell signaling	Cat#81464
anti-β-TrCP	Cell signaling	Cat#11984
anti-β-actin	Cell signaling	Cat#4970
anti-Caspase-3	Cell signaling	Cat#9662
normal rabbit IgG	Cell signaling	Cat#2729
anti-LC3B	Invitrogen	Cat#L10382
anti-Trim27	MyBiosource	Cat#MBS1492534
anti-Pan crotonylLysine	PTM Biolabs	Cat#PTM-515RM
Biological samples		
Leukapheresis from HIV-infected individuals	University of North Carolina Hospital	N/A
Chemicals, peptides, and recombinant proteins		
AZD5582	ChemieTek	CT-A5582
Crotonate acid	Sigma	113018-500G
Critical commercial assays		
NE-PER™ Nuclear and Cytoplasmic Extraction Reagents	Thermo Scientific	Cat#78835
NP40 cell lysis Buffer	Invitrogen	Cat#FNN0021
Protease Inhibitor Cocktail powder	Millipore Sigma	Cat#P5714
Protease/Phosphatase Inhibitor Cocktail (100X)	Cell signaling	Cat#5872
RNeasy mini kit	Qiagen	Cat#74106
DNase I	Invitrogen	Cat#18047019
SuperScript™ III Reverse Transcriptase	Invitrogen	Cat#18080093
TaqMan™ Universal PCR Master Mix	ABI	Cat# 4304437
Accell Delivery Media	horizon	Cat ID:B-005000-100
Pierce™ Protein A/G Agarose	Thermo Scientific	Cat#20421
EasySep™ Human CD4+ T Cell Enrichment Kit	Stemcell Tech.	Cat#19052
Custom EasySep™ Human Resting CD4+ T Cell Isolation Kit	Stemcell Tech.	N/A

(*Continued on next page*)

Continued

REAGENT or RESOURCE	SOURCE	IDENTIFIER
LIVE/DEAD™ Fixable Far Red Dead Cell Stain Kit	Invitrogen	Cat#L34973
Experimental models: Cell lines		
Jurkat	ATCC	TIB-152
2D10	Dr. Jonathan Karn	N/A
J-Lat A1	NIH HIV Reagent Program	N/A
J-Lat 10.6	NIH HIV Reagent Program	N/A
U1	NIH HIV Reagent Program	N/A
Experimental models: Organisms/strains		
Primary CD4+ T cell model of latency	Browne Lab	Bradley et al., 2018
Oligonucleotides		
HIV long LTR probe: 6FAMCCA GAG TCA CAC AAC AGA CGG GCA CAT AMRA	Invitrogen	Yukl, et al. 2018
HIV long LTR sense: GCC TCA ATA AAG CTT GCC TTG A	Invitrogen	Yukl, et al. 2018
HIV long LTR antisense: GGG CGC CAC TGC TAG AGA	Invitrogen	Yukl, et al. 2018
GAPDH (Hs99999905_m1)	Thermo Scientific	Cat#4331182
TRIM27	Applied Biosystems	Hs01100632_ml
p100/NFKB2	Applied Biosystems	Hs01028890_gl
Human TBP (TATA-box binding Protein) Endogenous Control	Applied Biosystems	Cat#4333769F
Trim 27 Accell small interfering RNAs	Dharmacon	Cat#E-006552-00-0020
scrambled control siRNAs	Dharmacon	Cat#D-001910-10-20
Software and algorithms		
GraphPad Prism 8	GraphPad Software Inc.	https://www.graphpad.com/
FlowJo v9	BD	https://www.flowjo.com/
Other		
Patient cell study	Study was approved by the University of North Carolina Institutional Review Board	UNC IRB committee

RESOURCE AVAILABILITY

Lead contact

Further information and requests for resources and reagents should be directed to the Lead Contact, Dr. Guochun Jiang (Guochun_Jiang@med.unc.edu). This study did not generate new unique reagents.

Materials availability

Materials described in this paper are available for distribution under the Uniform Biological Material Transfer Agreement, which was developed by the NIH to simplify the transfer of biological research materials.

Data and code availability

All the data associated with this work have been included in this article. This study did not generate any original code. Any additional information required to reanalyze the data reported in this paper is available from the lead contact upon request.

EXPERIMENTAL MODEL AND SUBJECT DETAILS

Cell models

2D10, J-Lat A1 cells, J-Lat 10.6 and U1 model of HIV latency were cultured in RPMI 1640 medium with 10% fetal bovine serum (FBS) and 1% penicillin streptomycin (Pen-Strep) in a 37°C incubator containing 5% CO2 (43, 44). J-Lat A1 cells, J-Lat 10.6, or U1 cells were from NIH AIDS Reagents Repository, 2D10 cell model of latency was a gift from Dr. Jonathan Karn (Case Western University, Cleveland, OH), which harbors a single copy of HIV-1pNL4-3 whose genome lacks sequences encoding the majority of the Gag-Pol polyprotein, but encompasses the full-length 5 and 3′ LTRs. It includes a gene encoding the marker protein green fluorescent protein (GFP) replacing Nef protein (Pearson et al., 2008). Primary CD4+ T cell model of latency was also used, which has been described in details (Bradley et al., 2018). Multiple HIV latency models were tested because, as thus far, there is not a single *in vitro* cell culture model available that captures all the features of HIV latency *in vivo*.

Primary CD4+ T cell isolation and cell-associated HIV gag RNA measurements

Leukapheresis samples were collected from HIV-infected individuals receiving suppressive antiretroviral therapy (ART). CD4+ T cells were isolated using the EasySep CD4+ T cells Enrichment Kit or a custom resting CD4+ T cells isolation kit (StemCell Technologies) as previously described (44, 46). The purified CD4+ T cells were plated at a density of $2x10^6$ cells and treated with indicated compounds. For the HIV gag RNA measurements in resting CD4+ T cells from ART-suppressed individuals, 3–5 replicates of 2–4 million resting CD4+ T cells per replicate were treated with compounds either for 24 or 48 hours. Cells were harvested, total RNA isolated and Gag HIV RNA measured as previously described after normalized with TBP internal control (Gay et al., 2020).

All participants provided informed consent and the study was approved by the UNC Institutional Review Board. The patient information, including age, gender, CD4+ T cell count, ART regimen and time under ART, have been included in Table 1.

Immunoblot analysis

Whole cell protein extract was prepared with NP40 cell lysis buffer containing proteinase inhibitors and phosphatase inhibitors (Sigma). Nuclear/cytoplasmic protein fractionation was achieved by NE-PER™ Nuclear and Cytoplasmic Extraction Reagents (Thermo Scientific, cat#, 78835). Protein expression of the canonical or non-canonical NF-κB signaling pathway and other HIV transcription-related pathways were evaluated by immunoblot using the corresponding antibody. Quantitation of protein levels was determined by densitometric scanning (Image Lab Software, Bio-Rad)

HIV gene expression by real-time PCR analysis or GFP flow cytometry

Total RNA was isolated using the RNeasy kit (Qiagen) followed by digestion with DNase I (Invitrogen). First-strand cDNA was synthesized using Superscript III (Invitrogen) with random primers (Invitrogen). Real-time PCR (TaqMan) was performed on an ABI QuantStudio 5 system using primers/probe sets purchased from ABI as previously reported (44, 46), where HIV was amplified with the early gag/long LTR region of HIV. The glyceraldehyde-3-phosphate dehydrogenase (GAPDH) and TBP primers/probe sets were used for control PCR (Applied Biosystems Inc.) HIV (GFP) was quantified by GFP expression using flow cytometry and the data were analyzed using FlowJo Software. Cell viability was evaluated using Live/Dead dye (Life Technologies) during flow cytometry.

Gene knockdown by small interfering RNA

2D10 cells or primary CD4+ T cells were plated in 96-well plates at $1x10^6$ cells/ml in Accell Delivery Media (Dharmacon). Accell small interfering RNAs (siRNAs) (E-006552-00-0020, Dharmacon) or its scrambled control siRNAs (D-001910-10-20, Dharmacon) were added to the cells at a final concentration of 1.5 μM. Cells were incubated with siRNA for 2 days. Cells were then re-suspended in RPMI 1640 medium with 10% fetal bovine serum (FBS), 1% penicillin streptomycin (Pen-Strep) and 10% FBS complete with 5 nM AZD5582. Cells were harvested after 24 hours. Then, RNA and protein were isolated.

Co-immunoprecipitation

Immunoprecipitations (IP) were performed as before (Li et al., 2012). Briefly, treated or untreated 2D10 cells were washed and lysed in 150 mM NaCl, 50 mM Tris-HCl (pH 7.2), 0.5% NP-40, and protease inhibitor

cocktail (Cell Signaling) followed by an incubation at 4°C for 20 min with vortex. Clarified lysates were pre-cleared with protein A/G agarose beads (Thermo Scientific), followed by IP with either anti-USP7 monoclonal antibody (Bethyl), anti-TRIM27 polyclonal antibody (MyBioSource), or normal rabbit IgG (Cell Signaling). IP was analyzed by sodium dodecyl sulfate-polyacrylamide gel electrophoresis (SDS-PAGE) and immunoblotting with 1st antibodies of anti-USP7 or anti-Trim27 antibody and 2nd antibodies of horseradish peroxidase-conjugated secondary antibody, followed by chemiluminescence detection (Amersham).

Sample preparation for quantitative proteomic analysis

One million of 2D10 cells were treated with or without 30 mM NaCr for 6 hours. Whole cell protein extracts were prepared with RIPA buffer (Sigma) followed by Co-IP with IgG or anti-PanCrotonylLysine antibody (PTM biolabs). The immune-complexes were prepared by Immunoprecipitation Dynabeads Kit and eluted by boiling in 20 μl SDS-PAGE sample buffer at 95°C for 5 minutes. The complex protein were further fractionated on a 10% SDS-PAGE gel and tryptic digested into peptides overnight at 37°C. Three biological replicates were prepared for this experiment.

Mass spectrometry analysis

Peptides were cleaned up by C18 stage tips. The clean peptides were dissolved in 0.1% formic acid and analyzed on a Q-Exactive HF-X coupled with an Easy nanoLC 1200 (Thermo Fisher Scientific, San Jose, CA). 5 μL of peptides were loaded on to an Acclain PepMap RSLC C18 Column (250 mm × 75 μm ID, C18, 2 μm, Thermo-Fisher). Analytical separation of all peptides was achieved with 30 min gradient. A linear gradient of 5 to 30% buffer B over 17 min was executed at a 300 nl/min flow rate followed a ramp to 40% B in 3 min, and 10-min wash with 100% buffer B, where buffer A was aqueous 0.1% formic acid, and buffer B was 80% acetonitrile and 0.1% formic acid.

LC-MS experiments were performed in a data-dependent mode with full MS (externally calibrated to a mass accuracy of <5 ppm and a resolution of 60,000 at m/z 200) followed by high energy collision-activated dissociation-MS/MS of the top 20 most intense ions with a resolution of 15,000 at m/z 200. High energy collision-activated dissociation-MS/MS was used to dissociate peptides at a normalized collision energy of 27 eV in the presence of nitrogen bath gas atoms. Dynamic exclusion was 30.0 seconds. There were two biological replicates for one treatment and each sample was subjected to two technical LC-MS replicates.

MS data analysis

Mass spectra processing and peptide identification were performed on the Andromeda search engine in MaxQuant software (Version 1.6.0.16) against a human UniProt database (UP000005640). All searches were conducted with a defined modification of cysteine carbamidomethylation, with methionine oxidation and protein amino-terminal acetylation as dynamic modifications. Peptides were confidently identified using a target-decoy approach with a peptide false discovery rate (FDR) of 1% and a protein FDR of 1%. A minimum peptide length of 7 amino acids was required, maximally two missed cleavages were allowed, initial mass deviation for precursor ion was up to 7 ppm, and the maximum allowed mass deviation for fragment ions was 0.5 Da. Data processing and statistical analysis were performed on Perseus (Version 1.6.0.7). Protein quantitation was performed on biological replicate runs, and a two-sample T-test statistics was used to report statistically significant expression fold-changes.

QUANTIFICATION AND STATISTICAL ANALYSIS

Bliss independent analysis

Synergy of crotonate with AZD5582 in latency reversal was calculated by the Bliss independence analysis (Jiang et al., 2018; Laird et al., 2015). All the values were normalized with the percentage of GFP+ cells reactivated by PMA. For drugs x and y, the predicted fraction affected by the combination of drug x and drug y (faxyP) is defined as the equation faxyP = fax +fay−(fax)(fay), where the observed values of individual drug x is fax and drug y was fay. The observed combination effect (FaxyO) is the value when both drug x and drug y are tested together. Using this model, Δfaxy = faxyO-faxyP defines the synergy if Δ faxy > 0, additive effect if Δ faxy = 0, or antagonism if Δ faxy < 0. Statistical significance was determined using a two-tailed t-test to compare faxyO with faxyP, where *, $p<0.05$ was considered significant.

Other statistical analyses

Means and standard errors (SEs) were calculated for all data points from at least 3 independent experiments. Statistical significance was determined using the two-tailed Student T test or One-way ANOVA test, where *, $p < 0.05$ was considered significant. GO functional enrichment was performed by using software tool FunRich (funrich.org).